DOI: 10.1021/ma902099c

Macromolecules
ARTICLE

Degradable Amphiphilic End-Linked Conetworks with Aqueous Degradation Rates Determined by Polymer Topology

Maria D. Rikkou,[†] Elena Loizou,[†] Lionel Porcar,[‡] Paul Butler,[§] and Costas S. Patrickios*,[†]

[†]*Department of Chemistry, University of Cyprus, P.O. Box 20537, 1678 Nicosia, Cyprus,* [‡]*Institut Laue-Langevin, B. P. 156, F-38042 Grenoble, Cedex 9, France, and* [§]*Center for Neutron Research, National Institute of Standards and Technology, Bldg 235, E151, 100 Bureau Drive STOP 6102, Gaithersburg, Maryland 20899-6102*

Received September 22, 2009; Revised Manuscript Received November 2, 2009

ABSTRACT: Degradable amphiphilic conetworks, based on end-linked amphiphilic ABA triblock copolymers with a labile fragment in the middle, were synthesized by sequential group transfer polymerization (GTP) of monomers and cross-linker, using a GTP bifunctional initiator containing two hemiacetal ester cleavable groups. The degrees of swelling (DSs) in tetrahydrofuran (a nonselective solvent) of most conetworks span a range of values from 15 to 18, whereas the sol fraction ranged between 27 and 42% in most cases. The labile groups of the initiator fragment allowed for the facile, site-specific conetwork cleavage in pure water and alcohols at a rate that depended on polymer architecture and composition. A systematic investigation was performed by following in detail the temporal evolution of the swollen mass of the conetworks in water and methanol. Most interestingly, a particular conetwork presented a maximum in its swelling profile with time both in water ($DS_{max} \sim 20$) and in methanol ($DS_{max} \sim 30$) due to the simultaneous occurrence of swelling and degradation. A small-angle neutron scattering (SANS) study of the conetworks in deuterated water enabled the independent monitoring of conetwork swelling and degradation as these two processes appeared as two separate peaks in the SANS profiles, the former of which being related to the self-organization of the hydrophobic blocks within the conetworks, whereas the latter being connected with the correlations among the amphiphilic star block copolymers released in solution during the course of conetwork hydrolysis.

Introduction

Amphiphilic polymer conetworks (APCNs) are modern cross-linked materials comprising hydrophilic and hydrophobic monomer repeating units.[1] When the hydrophobic units are arranged in relatively long segments, with degrees of polymerization (DPs) typically 10 or higher, these materials self-assemble in aqueous media, yielding collapsed hydrophobic nanophases and water-swollen hydrophilic nanophases.[2] These nanostructured APCNs are most appropriate for an increasing number of technological[3] and biomedical[4] applications. Recognizing that polymer perfection is instrumental for better nanophase separation, our research team has been working for the past 10 years for the development of APCNs based on end-linked amphiphilic ABA triblock copolymers.[5] In our studies, we explored various combinations of hydrophilic and hydrophobic monomer repeating units as well as a range of copolymer molecular weights, block ratios, and architectures.[6] We also characterized the resulting APCN morphologies using scattering and microscopy techniques.[7]

Degradable polymers constitute another important branch of polymer science, with applications in microelectronics (polymeric resists) and medicine (resorbable surgical sutures, scaffolds for tissue engineering, and matrices for drug and protein delivery). Although the vast majority of degradable polymers is based on *degradable monomer repeating units* (e.g., copolymers of lactic and glycolic acids),[8] there is an increasing number of branched polymers bearing *degradable cross-links*.[9,10] Polymers bearing *degradable initiator residues* are even more rare, with only a handful of examples,[11] all of which were recently reported and all concerned bifunctional initiators of atom transfer radical polymerization (ATRP).[12] Although the design and preparation of such initiators are difficult, they constitute a powerful tool in the hands of the macromolecular engineer, providing the capability for chain cleavage at a precisely defined location, in the middle of the chain, leading to the cutting of the structure exactly in half.

Introduction of degradability in APCNs would enhance their functionality and extend their application potential. This was exactly the aim of this investigation. The APCNs produced in this study were well-defined, as they were based on end-linked amphiphilic triblock copolymers. Polymer synthesis was performed using group transfer polymerization (GTP)[13,14] and sequential monomer and cross-linker additions onto a bifunctional initiator. Degradability was introduced through the initiator, resulting in a labile site located in the middle of the polymer chain and, therefore, at the center of the middle block. This precise arrangement, along with the well-established nanophase separation of APCNs in water, is expected to yield materials with interesting properties which can be accurately correlated to the composition and the architecture of the linear precursor chains.

Experimental Section

Materials and Methods. All chemicals were purchased from Aldrich, Germany. The reagents used for the synthesis of the conetworks were the monomers, 2-(dimethylamino)ethyl methacrylate (DMAEMA or D, hydrophilic, 98%) and methyl methacrylate (MMA or M, hydrophobic, 99%), and the cross-linker, ethylene glycol dimethacrylate (EGDMA or E,

*To whom correspondence should be addressed. E-mail: costasp@ucy.ac.cy.

 Published on Web 11/13/2009

hydrophobic, 98%). The degradable bifunctional initiator, 1,2-bis[1-(2-methyl-1-(trimethylsilyloxy)prop-1-enyloxy)ethoxy]-ethane (BisMTS), was synthesized according to our previously reported procedure.[15] The polymerization catalyst was tetrabutylammonium bibenzoate (TBABB), prepared as described by Dicker and co-workers.[14] It was stored under vacuum until use. The polymerization solvent was tetrahydrofuran (THF, analytical grade, 99.8%), which was dried by being refluxed over a sodium/potassium alloy for 3 days and was freshly distilled. The monomers and the cross-linker were passed through basic alumina columns and were stirred overnight over calcium hydride (90−95%) to remove the last traces of moisture and protic impurities. This was done in the presence of an added free radical inhibitor, 2,2-diphenyl-1-picrylhydrazyl hydrate (DPPH, 95%), to avoid undesired thermal polymerization. The monomers and the cross-linker were freshly distilled on a vacuum line (typical pressure ~0.1 mmHg) prior to the polymerization. Under the vacuum conditions used, MMA distilled over at room temperature and DMAEMA distilled at 35 °C, whereas EGDMA distilled at 80 °C.

Polymerizations. The polymerization procedure for the synthesis of the conetwork $EGDMA_1$-*b*-MMA_5-*b*-$DMAEMA_{20}$-I-$DMAEMA_{20}$-*b*-MMA_5-*b*-$EGDMA_1$ is described below. Freshly distilled THF (15.3 mL), 0.33 mL of BisMTS initiator (0.36 g, 0.83 mmol), and 5.55 mL of DMAEMA (5.18 g, 32.9 mmol) were transferred, in this order, into a 100 mL round-bottom flask sealed with a rubber septum, kept under an inert nitrogen atmosphere and containing TBABB catalyst (~10 mg, 20 μmol). A polymerization exotherm (28−41 °C) was immediately triggered which abated within 5 min. Samples were subsequently extracted to characterize the resulting polyDMAEMA by gel permeation chromatography (GPC) and ^{1}H NMR spectroscopy (monomer conversion = 100%: absence of high elution volume peak in the GPC trace and absence of signals from the olefinic protons in the ^{1}H NMR spectrum; polymer number-average molecular weight (MW) = M_n = 11 600 g mol^{-1}; polydispersity index = PDI = M_w/M_n = 1.18; M_w is the weight-average MW). Then, the second monomer, MMA (0.89 mL, 0.83 g, 8.32 mmol), was added slowly, giving an exotherm (35−39 °C). Samples were then withdrawn again and analyzed using GPC (monomer conversion = 100%; M_n = 14 600 g mol^{-1}; PDI = 1.16) and ^{1}H NMR spectroscopy (found 21.6 mol % MMA compared to 20.0 mol % theoretically expected). Finally, EGDMA (0.31 mL, 0.33 g, 1.64 mmol) was added, leading to gel formation within seconds. Conetworks of different compositions were prepared by varying the relative amounts of DMAEMA and MMA, whereas conetworks of different architectures were obtained by varying the order of reagent addition.

Characterization of the Conetwork Precursors and the Sol Fraction. *Gel Permeation Chromatography*. Samples of the homopolymer and the copolymer linear precursors obtained during the polymerizations and samples of the extractables from the conetworks were characterized using GPC to determine their MWs and their molecular weight distributions (MWD). GPC was performed on a Polymer Laboratories chromatograph equipped with an ERC-7515A refractive index detector and a PL Mixed "D" column. The mobile phase was THF modified with 2% triethylamine, delivered at a flow rate of 1 mL min^{-1} using a Waters 515 isocratic pump. The MW calibration curve was based on eight narrow MW (850, 2810, 4900, 11 550, 30 530, 60 150, 138 500, and 342 900 g mol^{-1}) linear polyMMA standards also from Polymer Laboratories.

^{1}H NMR Spectroscopy. The compositions of the linear conetwork precursors, the extractables from the conetworks, and the star (co)polymer resulting from the pure-water hydrolysis of the (co)networks were determined by ^{1}H NMR spectroscopy using a 300 MHz Avance Bruker NMR spectrometer equipped with an Ultrashield magnet. In the case of the linear precursors and the extractables the solvent was $CDCl_3$ containing traces of tetramethylsilane (TMS) which was used as an internal reference, whereas in the case of the star (co)polymers the solvent was CD_3OD. ^{1}H NMR spectroscopy in $CDCl_3$ was also used to follow the kinetics of the alcoholysis of a low MW, model compound related to the initiator. Finally, ^{1}H NMR spectroscopy was used to confirm the structure and the purity of the BisMTS bifunctional initiator, the monomers, and the cross-linker.

Determination and Characterization of the Conetwork Sol Fraction. The resulting (co)networks were extracted with 200 mL of THF for 2 weeks to remove the sol fraction. Next, the resulting solution of the extracted polymer in THF was recovered by filtration, and the solvent was subsequently evaporated off using a rotary evaporator. The recovered polymer was further dried for 2 days in a vacuum oven at room temperature. The sol fraction was calculated as the ratio of the dried mass of the extracted polymer divided by the theoretical mass of the polymer in the conetwork, estimated as the sum of the masses of the monomers (monomer conversion was 100% in all cases), the cross-linker, and the initiator used for the synthesis. The extractables were also characterized in terms of their MW and composition using GPC and ^{1}H NMR spectroscopy, respectively, as described above.

Measurement of the Conetwork Degrees of Swelling in THF. After extraction of the sol fraction, pieces from each THF-equilibrated (co)network were cut and weighed. Subsequently, each piece was dried in a vacuum oven at room temperature for 3 days and was reweighed. The degree of swelling (DS) was calculated as the ratio of the swollen divided by the dry (co)network mass.

Measurement of the Conetwork Apparent Degrees of Swelling in Water and Methanol. For the measurements of the apparent DSs as a function of time, a dry sample from each (co)network (~55 mg) was placed in a glass vial and ~5 mL of the proper solvent (water, deuterium oxide, or methanol) was added. The measurements were performed at room temperature (~23 °C), and in the case of the experiments in water, the pH was around 7.3, a result of the presence of the weakly basic DMAEMA units in the (co)networks. At regular time intervals, the solvent was removed via a disposable syringe, and the mass of the gel was determined gravimetrically. The apparent DSs at different times were calculated again as the ratio of the swollen divided by the dry (co)network mass. Finally, the moment of complete (co)network dissolution was noted.

Characterization of the Conetwork Hydrolysis Products. The hydrolysis products of all DMAEMA-containing (co)networks were insoluble in THF, even the ones hydrolyzed in pure water or alcohols. Thus, their GPC characterization was attempted in *N*,*N*-dimethylformamide (DMF) where these polymers were soluble. However, DMF was not capable of eluting the DMF-soluble star polymers which were retained on to the GPC column. Thus, the mobile phase was modified by the addition of potassium hexafluorophosphate (0.1 and 0.5 M), but, again, without any success regarding polymer elution. Information regarding the star polymer size was obtained only for the MMA star homopolymer, which was the hydrolysis (in HCl aqueous/THF solution) product of the MMA homopolymer end-linked network from our previous publication.[15] Further size information was obtained from the size characterization of DMAEMA−MMA star copolymers prepared directly using a monofunctional GTP initiator.

The compositions of the star polymer hydrolysis products obtained from the aqueous hydrolysis of the four water-cleavable (co)networks were determined using ^{1}H NMR spectroscopy in CD_3OD where these polymers were soluble. After hydrolysis, for NMR sample preparation, the star polymers were freeze-dried from water.

Bis(hemiacetal ester) Alcoholysis Kinetics. The alcoholysis kinetics of a model, low MW compound was studied using ^{1}H NMR spectroscopy. The model compound was the bis-(hemiacetal ester) precursor to the degradable bifunctional initiator, 1,2-bis[1-(2-methylpropionyloxyl)ethoxy]ethane. The

alcohols investigated were methanol, ethanol, 1-propanol, and 1-butanol. Attempts to follow the hydrolysis kinetics of the model compound by water were unsuccessful due to the very high rate of the reaction with water. In a typical alcoholysis experiment, a solution of ~30 mg of the bis(hemiacetal ester) (103 μmol) in 0.35 mL of $CDCl_3$ was prepared and transferred into an NMR tube. Then, 0.05 mL of a 0.5 M alcohol (dried and freshly distilled from calcium hydride) solution (25 μmol) was added to the same NMR tube. The contents of the tube were immediately mixed by the inversion of the tube which was placed in the spectrometer to follow the reaction by recording the ^{1}H NMR spectra at regular time intervals. The progress of the reaction was quantified by comparing the areas due to the signals of the newly formed (regular) acetal protons at 4.6 ppm to those of the original hemiacetal ester at 5.9 ppm. The concentration of the remaining alcohol was also necessary for the calculations. In the case of methanol, its instantaneous concentration could be directly calculated from the signal of the methanol methyl protons at 3.45 ppm in the ^{1}H NMR spectra. For the higher alcohols, due to the overlap of all the protons of all the alcohols with those of the bis(hemiacetal ester), the alcohol concentration was calculated from the amount of alcohol initially introduced into the system, and the concentration of produced acetal was determined from the ^{1}H NMR spectra. The data were fitted to second-order reaction kinetics from which the second-order alcoholysis rate constants were calculated.

Small-Angle Neutron Scattering (SANS). SANS measurements were performed on the 30 m NG7 instrument at the Center for Neutron Research of the National Institute of Standards and Technology (NIST). The incident wavelength was $\lambda = 6$ Å. One sample to detector distance of 4 m was employed, covering a q-range [$q = 4\pi/\lambda \sin(\theta/2)$] from 0.1 nm^{-1} < q < 1.5 nm^{-1}. The samples were loaded in 2 mm and 4 mm gap thickness quartz cells. In a typical experiment, 8 mg of dry (co)network was transferred into a quartz cuvette containing 1.5 mL of D_2O. The scattering intensity was recorded at regular time intervals. The scattering patterns were isotropic, and, therefore, the measured counts were circularly averaged. The averaged data were corrected for empty cell and background. The distance between the scattering centers was estimated from the position of the intensity maximum, q_{max}, as $2\pi/q_{max}$.

Results and Discussion

Synthetic Strategies and Conetwork Functionalities. The produced polymer conetworks clearly constitute an advance with regard to both our research team's synthetic objectives and those of other teams. Regarding the former, this is the first time we combine amphiphilicity with degradability; in the past, we synthesized and studied well-defined APCNs which were not degradable[5−7] and well-defined degradable networks which were not amphiphilic.[10,15] Regarding the latter, although end-linked networks based on degradable initiators have already been reported, these were composed of only hydrophobic homopolymers,[11d,e] whereas reported degradable APCNs comprised degradable monomer repeating units either in the macro-cross-linker[16a] or in the main chain.[16b] Although both controlled radical and anionic polymerization methods have been employed for the preparation of end-linked APCNs,[5−7] we elected the latter method because of the narrower MWD of the resulting precursor chains. In particular, we chose GTP,[13,14] a rapid, quasiliving anionic polymerization technique taking place at room temperature, best-suited for methacrylates. MMA and DMAEMA were employed as the hydrophobic and the hydrophilic comonomers, respectively, while EGDMA served as the cross-linker in this investigation. A tetraacetal bifunctional degradable GTP initiator, BisMTS,[15] bearing

Scheme 1. Synthesis of an APCN Based on End-Linked ABA Triblock Copolymers, Using the Degradable Bifunctional GTP Initiator[a]

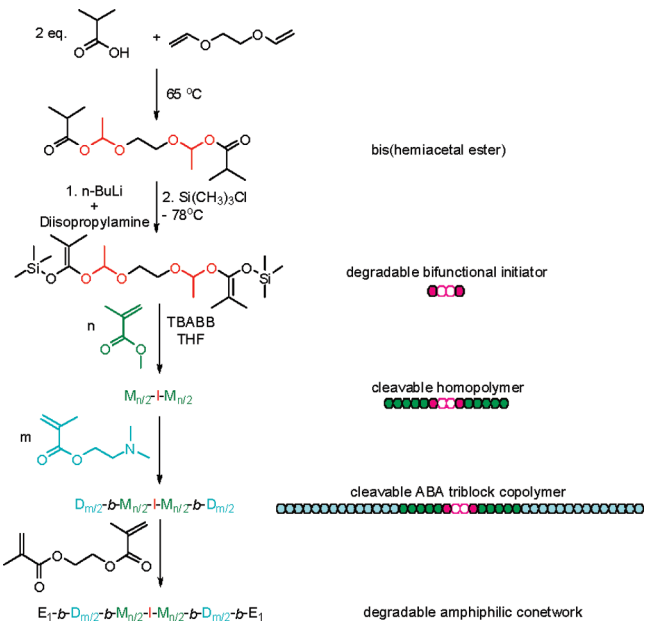

[a] The synthesis of the degradable bifunctional initiator is also shown on the top of the scheme. The green and blue colors represent the MMA (M) and the DMAEMA (D) units, respectively. The EGDMA (E) cross-linker units are shown in black. The degradable bifunctional initiator residue is presented with red color.

two silyl ketene acetal initiating groups and two degradable hemiacetal ester groups, was used for the sequential polymerization of the two comonomers and the cross-linker for the one-pot synthesis of the cleavable APCNs, as illustrated in Scheme 1.

Conetwork Compositions and Architectures. Conetworks of different compositions were afforded by varying the relative loadings of the two comonomers, whereas APCNs of different architectures were attained by changing the order of monomer and initiator additions. Nine (co)networks were prepared in total, from which three were homopolymer networks and six were copolymer conetworks. Two of the homopolymer networks were based on DMAEMA (with linear precursors of different MWs) and one on MMA. The conetworks included three samples based on DMAEMA-*b*-MMA-*b*-DMAEMA triblock copolymers ("ABA structure") of different compositions and three isomeric samples of the same composition but different architecture: one based on a MMA-*b*-DMAEMA-*b*-MMA triblock copolymer ("BAB structure"), one based on a DMAEMA-*co*-MMA statistical copolymer, and the randomly cross-linked conetwork of the statistical copolymer (prepared by the simultaneous terpolymerization of the two comonomers and the cross-linker). Also isomeric to these three samples was one of the three conetworks with the DMAEMA-*b*-MMA-*b*-DMAEMA structure. Thus, there were in total four isomeric conetworks with the same composition and different architecture. Schematic representations of all the (co)networks are illustrated in Figure 1.

Molecular Weights and Compositions of the Linear (Co)network Precursors. Table 1 lists the chemical structures of the linear homopolymer and copolymer precursors to the prepared (co)networks and displays their M_n and PDI values as well as their compositions, as determined using GPC and ^{1}H NMR spectroscopy, respectively. The linear precursors were homogeneous in terms of their size with relatively low PDIs, below 1.25 in most cases. The compositions of the

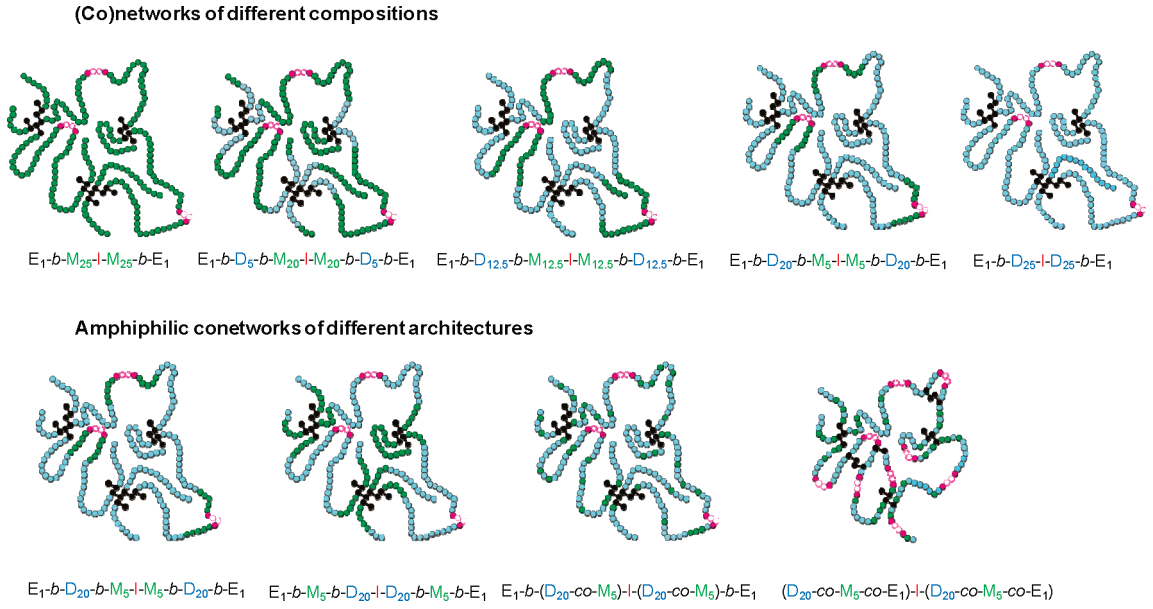

Figure 1. Schematic representations of the structures of the (co)networks synthesized in this study. The green and blue colors represent the MMA (M) and the DMAEMA (D) units, respectively. The EGDMA (E) cross-links are shown as black dumbbells. The degradable bifunctional initiator residue is presented with red color.

Table 1. Chemical Structures, Molecular Weights, Polydispersity Indices, and Compositions of the Linear Homopolymer and Copolymer Precursors to the Synthesized (Co)networks

		GPC results		^{1}H NMR
no.	polymer chemical structure[a]	M_n (g mol^{-1})	PDI	M (mol %)
1	D_{10}-I-D_{10}	6300	1.14	0.0
2	D_{25}-I-D_{25}	15700	1.15	0.0
3	M_{25}-I-M_{25}	9100	1.17	100.0
4a	D_{20}-I-D_{20}	11600	1.18	0.0
4b	E_1-*b*-M_5-*b*-D_{20}-I-D_{20}-*b*-M_5-*b*-E_1	14600	1.16	21.6
5a	M_5-I-M_5	2820	1.46	100.0
5b	D_{20}-*b*-M_5-I-M_5-*b*-D_{20}	20700	1.24	19.0
6	(D_{20}-*co*-M_5)-I-(D_{20}-*co*-M_5)	14200	1.16	21.0
7[b]	(D_{20}-*co*-M_5-*co*-E_1)-I-(D_{20}-*co*-M_5-*co*-E_1)			
8a	$M_{12.5}$-I-$M_{12.5}$	5180	1.19	100.0
8b	$D_{12.5}$-*b*-$M_{12.5}$-I-$M_{12.5}$-*b*-$D_{12.5}$	11700	1.30	48.5
9a	M_{20}-I-M_{20}	6360	1.21	100.0
9b	D_5-*b*-M_{20}-I-M_{20}-*b*-D_5	8400	1.23	81.0

[a] E: EGDMA, D: DMAEMA, M: MMA, I: initiator residue. [b] No linear precursor available as the three-dimensional conetwork is formed immediately.

Table 2. Mass Percentage, Molecular Weights, and Compositions of the Extractables from the (Co)networks As Measured by Gravimetry, GPC, and ^{1}H NMR Spectroscopy

			GPC results		^{1}H NMR
no.	(co)network chemical structure[a]	extractables (w/w %)	M_n	PDI	M (mol %)
1	E_1-*b*-D_{10}-I-D_{10}-*b*-E_1	54	1200	1.03	0.0
2	E_1-*b*-D_{25}-I-D_{25}-*b*-E_1	48	6950	1.37	0.0
3	E_1-*b*-M_{25}-I-M_{25}-*b*-E_1	42	6580	1.24	100
4	E_1-*b*-M_5-*b*-D_{20}-I-D_{20}-*b*-M_5-*b*-E_1	41	6340	1.28	17
5	E_1-*b*-D_{20}-*b*-M_5-I-M_5-*b*-D_{20}-*b*-E_1	37	6210	1.36	41
6	E_1-*b*-(D_{20}-*co*-M_5)-I-(D_{20}-*co*-M_5)-*b*-E_1	39	5500	1.22	28
7	(D_{20}-*co*-M_5-*co*-E_1)-I-(D_{20}-*co*-M_5-*co*-E_1)	23	7340	1.14	10
8	E_1-*b*-$D_{12.5}$-*b*-$M_{12.5}$-I-$M_{12.5}$-*b*-$D_{12.5}$-*b*-E_1	28	4290	1.27	82
9	E_1-*b*-D_5-*b*-M_{20}-I-M_{20}-*b*-D_5-*b*-E_1	27	5760	1.64	86

[a] E: EGDMA, D: DMAEMA, M: MMA, I: initiator residue.

copolymers were determined from the ^{1}H NMR spectra by ratioing the signal from the three methoxy protons (3.6 ppm) in MMA to the six protons in the two azamethyl groups (2.3 ppm) in DMAEMA and were found to be very close to the compositions calculated on the basis of the comonomer feed ratios. This was an expected agreement, given the complete monomer conversions in all polymerizations.

Conetwork Sol Fraction. Table 2 lists the sol fractions of all the (co)networks, which span a range of values from 23 to 54%, but most of them ranged between 27 and 42%. The lowest value, 23%, was presented by the randomly cross-linked contework. GPC measurements indicated that the sol fraction mainly consisted of linear chains with MWs lower than those of the corresponding linear precursors (in some

Table 3. (Co)network Degrees of Swelling in THF Determined Gravimetrically

no.	(co)network chemical structure[a]	DS in THF
1	E_1-*b*-D_{10}-I-D_{10}-*b*-E_1	6.9 ± 1.9
2	E_1-*b*-D_{25}-I-D_{25}-*b*-E_1	22.7 ± 2.5
3	E_1-*b*-M_{25}-I-M_{25}-*b*-E_1	6.2 ± 3.3
4	E_1-*b*-M_5-*b*-D_{20}-I-D_{20}-*b*-M_5-*b*-E_1	15.5 ± 3.5
5	E_1-*b*-D_{20}-*b*-M_5-I-M_5-*b*-D_{20}-*b*-E_1	15.0 ± 1.3
6	E_1-*b*-(D_{20}-*co*-M_5)-I-(D_{20}-*co*-M_5)-*b*-E_1	17.9 ± 5.6
7	(D_{20}-*co*-M_5-*co*-E_1)-I-(D_{20}-*co*-M_5-*co*-E_1)	7.8 ± 0.2
8	E_1-*b*-$D_{12.5}$-*b*-$M_{12.5}$-I-$M_{12.5}$-*b*-$D_{12.5}$-*b*-E_1	16.7 ± 1.5
9	E_1-*b*-D_5-*b*-M_{20}-I-M_{20}-*b*-D_5-*b*-E_1	16.5 ± 1.2

[a] E: EGDMA, D: DMAEMA, M: MMA, I: initiator residue.

cases even lower than those of the linear homopolymer precursors), suggesting that these resulted from termination at the early stages of the polymerization procedure. The same conclusion was also reached by examining the compositions of the extractables from the conetworks, which were found to be richer in the monomer that was added first during the sequential polymerization.

Conetwork Degrees of Swelling in THF. The conetworks were also characterized in terms of their degrees of swelling (DSs) in THF, and the results are listed in Table 3. The DSs in THF of most conetworks span a range of values from 15 to 18, a result of the behavior of THF as a nonselective solvent for DMAEMA and MMA and the similar molar masses of the precursor chains. In the case of the randomly cross-linked conetwork, a much lower value of 8 was displayed, suggesting a more efficient distribution of cross-linker in this sample. In the case of the two DMAEMA homopolymer networks, the DSs increased as the elastic chain length increased.

Conetwork Degradation in Pure Water and Alcohols. Before proceeding to hydrolysis by mineral acid, we decided to also measure the DSs of the (co)networks in water. To our surprise, many of the networks reproducibly dissolved, manifesting spontaneous hydrolysis by pure water. This is an unexpected and yet very important finding in this study. Dissolution took place in alcohols, too, albeit at a slower rate, and also in water−THF mixtures at a rate that depended on the water content of the mixture. The dissolution rate also depended on the conetwork type and mass. For example, pieces of ~200 mg of the $EGDMA_1$-*b*-$DMAEMA_{20}$-*b*-MMA_5-I-MMA_5-*b*-$DMAEMA_{20}$-*b*-$EGDMA_1$ dried conetwork required 0.5, 4, and 26 days to completely dissolve in water, methanol and ethanol, respectively, whereas it took them 1.5, 7, and 15 days to completely dissolve in 2:1, 1:1, and 1:2 v/v water−THF mixtures, respectively.

Intrigued by the above observations, we decided to perform a systematic investigation and follow in detail the temporal evolution of the swollen mass of the (co)networks in water and methanol. These apparent DSs would depend not only on the swelling properties of the initial (nonhydrolyzed) (co)networks but also on the degradation properties. In particular, as the networks degrade, their cross-link density decreases, leading to an increased solvent uptake. On the other hand, network degradation results in polymer detachment from the network with concomitant mass (polymer and accompanying solvent) loss and reduction in the apparent DS. We expect the former degradation effect (increase in apparent DS) to dominate in the earlier stages of the experiment, whereas the latter (decrease in apparent DS) in the later stages. Thus, the appearance of a maximum in the temporal evolution of the swelling profile is likely. The deconvolution of the concurrent swelling and degradation processes will be demonstrated for a triblock copolymer-based end-linked conetwork using SANS in a subsequent section of this article.

Figure 2a shows the swelling profiles in water of end-linked (co)networks of different compositions: three conetworks based on different DMAEMA-*b*-MMA-*b*-DMAEMA copolymers and the two DMAEMA and MMA homopolymer networks. Whereas the apparent DSs in water of the DMAEMA homopolymer end-linked network decreased very quickly and the network completely dissolved (due to the hydrolysis of the initiator residue) within less than 100 min (indicated by the vertical arrow at 85 min), the MMA homopolymer network and the two MMA-richest conetworks displayed low and time-invariant DSs, a result of the protection of the labile initiator residue from water by the surrounding long hydrophobic MMA blocks. Because of their increased hydrophobicity, these (co)networks swelled very little in water and did so according to their composition. The DMAEMA-rich copolymer end-linked conetwork was the most interesting and exhibited a swelling maximum: increasing apparent DS at the beginning due to a large initial water absorption and some conetwork hydrolysis, followed by a large decrease in the apparent DS due to extensive conetwork hydrolysis and dissolution at 200 min.

Figure 2b plots the swelling profiles in water of the four isomeric APCNs of different polymer architecture: the APCN based on the end-linked MMA-*b*-DMAEMA-*b*-MMA triblock copolymer, that based on the end-linked DMAEMA-*b*-MMA-*b*-DMAEMA triblock copolymer (replotted from Figure 2a), the one based on the end-linked DMAEMA-MMA statistical copolymer, and the randomly cross-linked APCN of the statistical copolymer. The MMA-*b*-DMAEMA-*b*-MMA-based conetwork exhibited decreasing apparent DSs and dissolved within 40 min, presenting similar behavior to the end-linked DMAEMA homopolymer network of Figure 2a. In this conetwork, the water-labile initiator residue is flanked by two water-soluble poly-DMAEMA segments, allowing the prompt access of water to the initiator residue which gets cleaved swiftly, before the conetwork can attain maximum swelling. This swelling behavior is to be contrasted to that of its isomer with the inverse block sequence, discussed in the previous paragraph (Figure 2a), in which the initiator residue was flanked by two hydrophobic polyMMA segments, restricting water access and delaying the hydrolysis of this conetwork. Thus, reversing the block sequence can largely influence the hydrolysis rates in these conetworks where the weak link is precisely placed in the middle of the chains. The apparent swelling profile of the end-linked conetwork based on the statistical copolymer was similar to that based on the triblock with a polyDMAEMA midblock but presented a slightly delayed full dissolution, at 50 min compared to 40 min in the case of the latter conetwork. As these isomeric APCNs are DMAEMA-rich, the initiator residue is mainly surrounded by DMAEMA units in the former conetwork, providing limited protection from hydrolysis. The presence of some hydrophobic MMA units (20 mol %) is the reason why dissolution was slightly delayed compared to the other APCN. Finally, the randomly cross-linked conetwork of the statistical copolymer gradually swelled without completely dissolving, as the initiator residues in this architecture were also protected by the hydrophobic EGDMA cross-linker units which were randomly distributed.

The apparent swelling profiles of all the (co)networks in methanol were also measured and are presented in Figure 3. In methanol, dissolution took place 1 order of magnitude more slowly, but the apparent swelling profiles were qualitatively very similar to those measured in water. Figure 3a plots

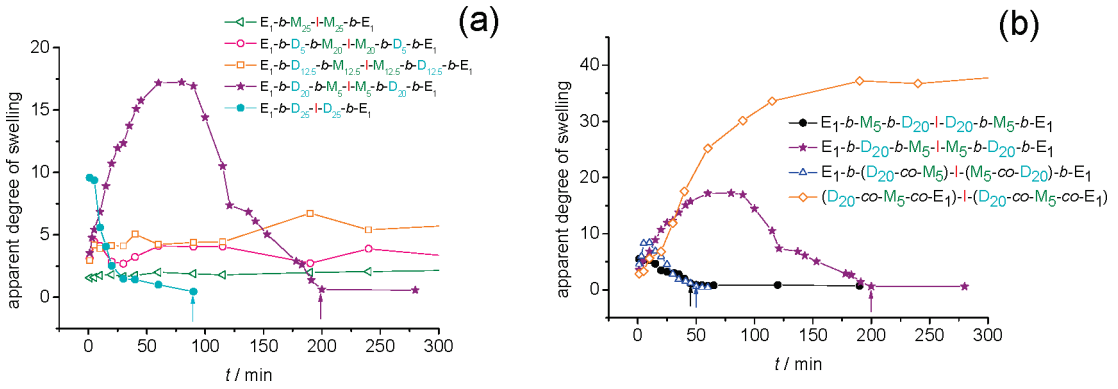

Figure 2. Temporal evolution of the apparent degrees of swelling of all the (co)networks in water: (a) effect of (co)polymer composition; (b) effect of copolymer architecture. The vertical colored arrows indicate the time at which complete (co)network dissolution was observed.

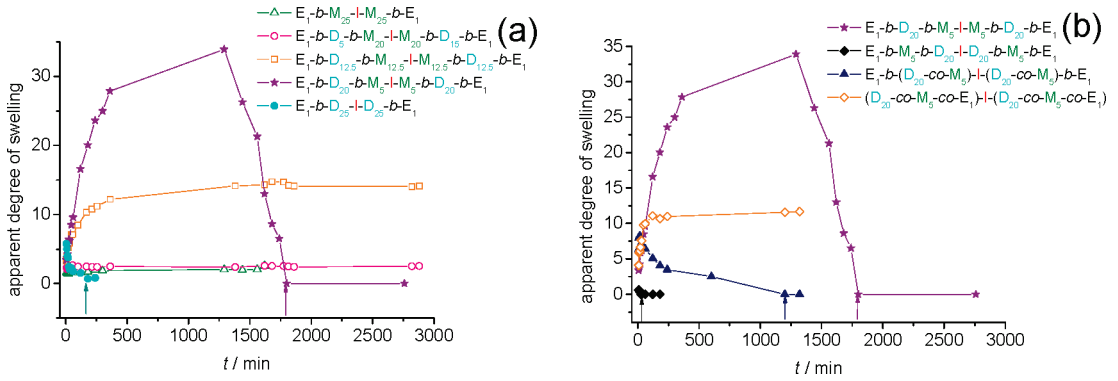

Figure 3. Temporal evolution of the apparent degrees of swelling of all the (co)networks in methanol: (a) effect of (co)polymer composition; (b) effect of copolymer architecture. The vertical colored arrows indicate the time at which complete (co)network dissolution was observed.

the swelling profiles in methanol of the of end-linked (co)networks of different compositions. The swelling profiles of these five networks are similar to the swelling profiles measured in water. The conetwork based on the DMAEMA$_{20}$-*b*-MMA$_{10}$-*b*-DMAEMA$_{20}$ triblock copolymer was again the most interesting one, exhibiting the anticipated maximum in its swelling behavior. This conetwork, bearing a low MMA content, exhibited a DS in methanol increasing to about 30 within the first 10 h and then decreasing to zero within 30 h (the vertical arrow at 1780 min indicates the point at which complete conetwork dissolution was observed). Figure 3b shows the effect of conetwork architecture on the kinetics of conetwork swelling and methanolysis. Again, the swelling profiles observed were qualitatively very similar to those measured in water.

Star Polymer Molecular Weights, Number of Arms, and Composition. The retention of the DMAEMA-containing star (co)polymers from the hydrolyzed (co)networks on to the GPC columns, even when the mobile phase was appropriately modified to secure star polymer solubility, did not allow the determination of their MWs and MWDs. This undesired retention was probably the result of the combination of the presence of the positively ionizable DMAEMA monomer repeating units and the negatively ionizable terminal isobutyric acid unit from the hydrolyzed initiator fragment. However, the MMA star homopolymer from the hydrolyzed (using aqueous HCl in THF) end-linked MMA homopolymer network smoothly eluted even in the original THF mobile phase, allowing the calculation of its relative and absolute MWs of M_n (GPC) = 39 700 g mol^{-1} and M_w (static light scattering) = 88 900 g mol^{-1} and finally yielding an (absolute) arm number of 18.[15] DMAEMA−MMA star copolymers with an arm DP of 25, synthesized independently using a monofunctional (nondegradable) GTP initiator (bearing no terminal carboxylic acid group), were similarly characterized and were determined to bear about 20 arms. Thus, all the star (co)polymers of the present study, resulting from the hydrolysis of end-linked (co)networks with precursor chains with a DP of 50, are believed to bear ~20 arms. Characterization using ^{1}H NMR in CD_3OD of the star (co)polymers obtained from the pure-water hydrolysis of the four water-cleavable (co)networks allowed the determination of their compositions which are listed in Table 4. The results show that the measured compositions were sufficiently close to those expected theoretically based on the comonomer feed ratios.

Table 4. Chemical Structures and Compositions of the Star (Co)polymers Obtained from the Aqueous Hydrolysis of the Four Water-Cleavable (Co)networks

no.	star (co)polymer chemical structure[a]	*M* (mol %)
2	D_{25}-*b*-E_1	0.0
4	D_{20}-*b*-M_5-*b*-E_1	24
5	M_5-*b*-D_{20}-*b*-E_1	32
6	(D_{20}-*co*-M_5)-*b*-E_1	24

[a] E: EGDMA, D: DMAEMA, M: MMA.

Alcoholysis Kinetics of a Low MW, Model Compound. To better understand the reaction of the cleavage of the initiator residue, we performed a systematic study on the alcoholysis (using methanol through 1-butanol) of a low MW compound with the same structure as that of the initiator residue in the polymers within the conetworks. This low MW compound was 1,2-bis[1-(2-methylpropionyloxyl)ethoxy]-ethane, the bis(hemiacetal ester) (Scheme 1) precursor to the initiator. Figure 4 shows some representative ^{1}H NMR spectra taken during the methanolysis of the hemiacetal ester

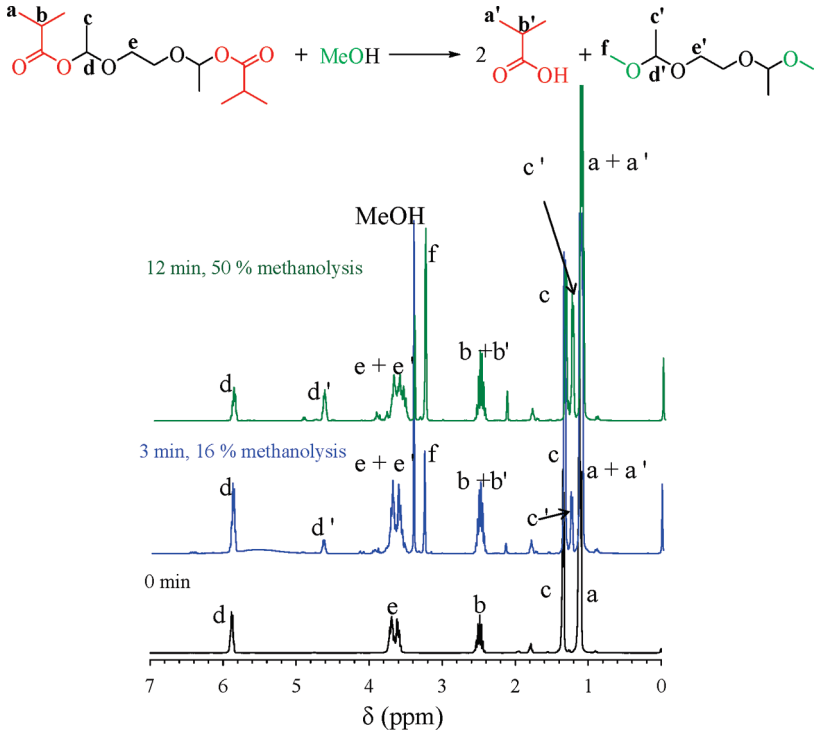

Figure 4. Proposed methanolysis reaction and ^{1}H NMR spectra taken during the methanolysis of 1,2-bis[1-(2-methylpropionyloxyl)ethoxy]ethane at different times.

at different times. As time goes by, two new peaks appear in the spectra, one at 4.6 ppm and one at 1.2 ppm, which can be assigned to the new bisacetal formed during methanolysis.

Figure 4 also displays the proposed reaction of methanolysis of the bis(hemiacetal ester) which is consistent with our ^{1}H NMR spectra. This reaction indicates that the main alcoholysis product was the bisacetal resulting from the substitution of isobutyric acid by the alcohol. The other alcoholysis product was isobutyric acid (manifested by its carboxylic acid protons at ~10 ppm in the ^{1}H NMR spectrum—region not covered in the presented spectra) rather than methyl isobutyrate, as the former compound appears to be a good leaving group. Thus, carboxylic acids can be protected using vinyl ethers and subsequently be deprotected using water or alcohol. Although such a protection has previously been used in polymer chemistry for carboxylic acid group protection in monomers[17a] and cross-linkers,[17b] to the best of our knowledge, deprotection using water or methanol has never been intentionally attempted, as the resulting polymers were, in most cases, hydrophobic and insoluble in water or methanol. However, there is one report where a vinyl ether was used to protect carboxylic acids in antibiotics synthesis, followed by the facile room temperature deprotection using water/methanol mixtures.[18]

The alcoholysis kinetics data with all four alcohols were fitted to second-order kinetics and shown in Figure S1 in the Supporting Information. The fits were very good, especially for the two lower alcohols, as indicated by the good linearity in the plots. From the fits, the second-order alcoholysis rate constants and the 95% confidence intervals were calculated and are listed in Table 5. The rate constants geometrically decreased with the alcohol size, from methanol to 1-propanol, indicating a severe slowdown of the alcoholysis reaction probably arising from increased steric hindrances. Thus, the rate of cleavage of the low MW bis(hemiacetal ester) and that of the polymer networks can also be adjusted by the appropriate choice of alcohol.

Table 5. Second-Order Alcoholysis Rate Constants of the Bis(hemiacetal ester) in Various Lower Aliphatic Alcohols

alcohol	k (M^{-1} min^{-1})
methanol	0.234 ± 0.017
ethanol	0.12 ± 0.03
1-propanol	0.05 ± 0.03
1-butanol	0.05 ± 0.02

Deconvolution of Conetwork Degradation and Swelling/Structure Formation. The structure of the four degradable networks upon swelling from the dried state in D_2O was studied using SANS. For the two triblock copolymer-based end-linked APCNs, this SANS study enabled the separation of conetwork degradation from the simultaneous swelling/hydrolysis processes. In particular, these two samples presented the most interesting profiles, with two clear, time-dependent peaks, whose intensity was enhanced by the nanophase separation of the polyMMA blocks in deuterium oxide (Figure 5a,b). The SANS profiles of the other two networks, the APCN based on the end-linked statistical copolymer (Figure 5d) and the DMAEMA homopolymer end-linked network (Figure 5d), presented only long tails and shallow shoulders due to lack of nanophase separation: in the former, the MMA units are randomly distributed and mixed with the hydrophilic DMAEMA units, not providing enough hydrophobic force to drive nanophase separation, whereas in the latter there are no hydrophobic units at all.

In the SANS profiles of the two triblock copolymer-based APCNs, there are two peaks which both grow in intensity with time, while their position remains approximately constant. The peak at higher q values (q_{max} = 0.6 nm^{-1}) corresponds to the separation of the polyMMA hydrophobic scattering centers within the conetworks at about 10 nm ($=2\pi/q_{max}$) and disappears at the later stages of the experiment due to complete conetwork dissolution. The particular separation at 10 nm (characteristic length) is consistent with the dimensions of the copolymer chains (contour length of

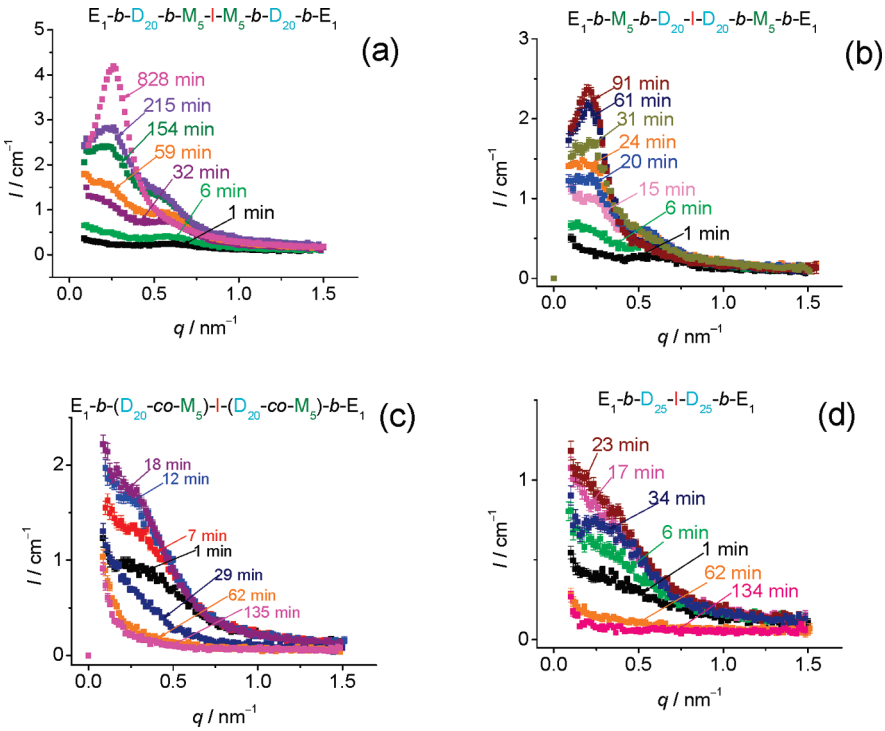

Figure 5. Time evolution of the SANS profiles of the four water-degradable (co)networks in D_2O: (a) $EGDMA_1$-*b*-$DMAEMA_{20}$-*b*-MMA_5-I-MMA_5-*b*-$DMAEMA_{20}$-*b*-$EGDMA_1$, (b) $EGDMA_1$-*b*-MMA_5-*b*-$DMAEMA_{20}$-I-$DMAEMA_{20}$-*b*-MMA_5-*b*-$EGDMA_1$, (c) $EGDMA_1$-*b*-($DMAEMA_{20}$-*co*-MMA_5)-I-($DMAEMA_{20}$-*co*-MMA_5)-*b*-$EGDMA_1$, and (d) $EGDMA_1$-*b*-$DMAEMA_{25}$-I-$DMAEMA_{25}$-*b*-$EGDMA_1$. The correlation peaks in (a) and (b) correspond to the spacing of the hydrophobic MMA scattering centers within the APCNs (0.6 nm^{-1}) and the spacing between the released amphiphilic star block copolymers in solution (0.2 nm^{-1}).

about 13 nm for a chain with a DP of 50). A closer examination of the position of this peak reveals a slight decrease in q_{max} with time, corresponding to an increase in the spacing from 10 to 12 nm and consistent with gradual conetwork swelling. The peak at lower q values (q_{max} = 0.2 nm^{-1}) corresponds to about 30 nm, which agrees well with the separation between the star polymers in solution (for this calculation, a star polymer MW of 100 000 g mol^{-1} and a star polymer concentration of 1% were assumed), resulting from the hydrolysis of the networks. A closer examination of the position of this peak reveals a slight increase in q_{max} with time, corresponding to a reduction in the spacing from 35 to 24 nm and consistent with a gradual increase in the star polymer concentration as network degradation progresses. This peak persists even after complete conetwork dissolution, and the relevant characteristic length increases if the experiment is repeated with a smaller amount of conetwork in a given volume of D_2O.

Because of the limited amount of APCN samples available, a gravimetric determination of the temporal evolution of the star polymer release profiles was precluded. Furthermore, chromatographic analysis was not possible either due to the retention of the star polymers on to the GPC column. Instead, an estimation of the time dependence of star polymer release was performed using the time-dependent SANS profiles for one of the triblock copolymer-based APCNs. In this treatment, a linear relationship between the SANS peak height (from the projected baseline of the SANS profile) and polymer concentration was assumed. Figure 6 presents the cumulative concentration of star block copolymer $DMAEMA_{20}$-*b*-MMA_5-*b*-$EGDMA_1$ released from the hydrolysis in D_2O of the parent APCN $EGDMA_1$-*b*-MMA_5-*b*-$DMAEMA_{20}$-I-$DMAEMA_{20}$-*b*-MMA_5-*b*-$EGDMA_1$. The release profile is sigmoidal and hydrolysis is completed within ~100 min.

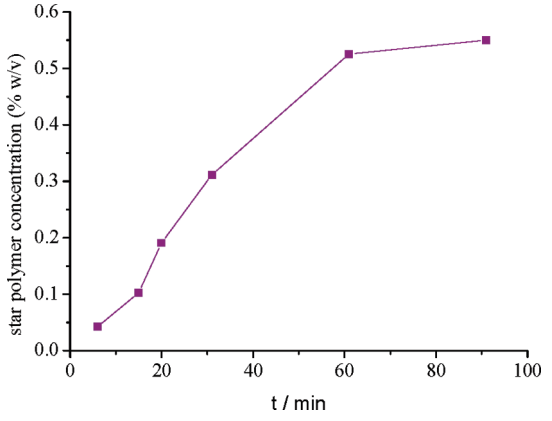

Figure 6. Release kinetics of star block copolymer $DMAEMA_{20}$-*b*-MMA_5-*b*-$EGDMA_1$ from the parent APCN hydrolyzed in D_2O.

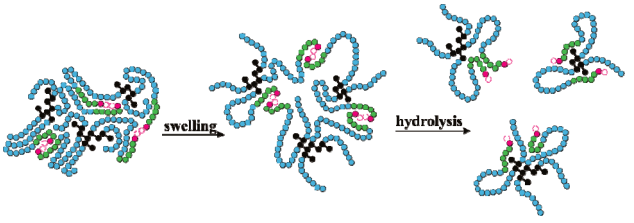

Figure 7. Schematic representation of the swelling, self-organization, and degradation processes occurring in an APCN in water, ultimately yielding aqueous solutions of amphiphilic star copolymers. Red: initiator residues; blue: hydrophilic monomer repeating units; green: hydrophobic monomer units; black: hydrophobic cross-linker units.

Figure 7 illustrates schematically the processes taking place when a piece of dried APCN based on the end-linked ABA triblock copolymer is transferred into water. First, the

conetwork, which is initially in the disordered state, starts absorbing water and swelling. At the same time, the polyMMA blocks try to hide from water and form hydrophobic nanophases, consistent with the peaks at higher q values in the SANS profiles. As the conetwork hydrolyzes, it produces a solution of star polymers in which the hydrophobic polyMMA blocks are aggregated, providing contrast in D_2O and giving rise to the peaks at lower q values. Although hydrolysis is slower than swelling in the two triblock APCNs, these two processes largely coexist, leading to the two scattering peaks observed in the SANS profiles.

Conclusions

In summary, a new, well-defined, end-linked conetwork system, combining degradability with amphiphilicity, is reported. The former functionality was conferred by the use of an appropriately designed initiator, whose labile groups allowed for facile, site-specific conetwork cleavage in pure water and alcohols. The latter functionality, imparted by the nature of the two comonomers, led to aqueous nanophase separation. SANS studies on degrading triblock APCNs in D_2O presented two peaks: one due to conetwork nanophase separation and the other due to the correlations between the amphiphilic star block copolymer degradation products. In a most interesting end-linked ABA triblock copolymer APCN, the temporal evolution of the aqueous and methanol swelling profiles presented a maximum due to the simultaneous occurrence of swelling and degradation. Owing to the surgical placement of the labile initiator fragments in the middle of the copolymer chains, the degradation rates highly depended on the conetwork architecture which determined the nanophase where degradation would occur.

Acknowledgment. We thank Cyprus Research Promotion Foundation and EU Structural and Cohesion Funds for Cyprus (Doctoral Research Grant PENEK2008 ENISX/ 0308/45 to M.D.R.), the University of Cyprus Research Committee, the A. G. Leventis Foundation (NMR spectrometer), and the National Institute of Standards and Technology and the U.S. Department of Commerce in providing the neutron research facilities used in this work.

Supporting Information Available: Second-order kinetic plots of the cleavage of the bis(hemiacetal ester) using the four alcohols. This material is available free of charge via the Internet at http://pubs.acs.org.

Note Added after ASAP Publication. This article posted ASAP on November 13, 2009. The Acknowledgment has been revised. The correct version posted on November 19, 2009.

References and Notes

(1) (a) Gitsov, I. *J. Polym. Sci., Part A: Polym. Chem.* **2008**, *46*, 5295–5314. (b) Erdodi, G.; Kennedy, J. P. *Prog. Polym. Sci.* **2006**, *31*, 1–18. (c) Patrickios, C. S.; Georgiou, T. K. *Curr. Opin. Colloid Interface Sci.* **2003**, *8*, 76–85.

(2) (a) Hu, Z.; Chen, L.; Betts, D. E.; Pandya, A.; Hillmyer, M. A.; DeSimone, J. M. *J. Am. Chem. Soc.* **2008**, *130*, 14244–14252. (b) Bruns, N.; Scherble, J.; Hartmann, L.; Thomann, R.; Iván, B.; Mülhaupt, R.; Tiller, J. C. *Macromolecules* **2005**, *38*, 2431–2438. (c) Scherble, J.; Thomann, R.; Iván, B.; Mulhaupt, R. *J. Polym. Sci., Part B: Polym. Phys.* **2001**, *39*, 1429–1436. (d) Georgiou, T. K.; Vamvakaki, M.; Patrickios, C. S. *Polymer* **2004**, *45*, 7341–7355. (e) Gitsov, I.; Zhu, C. *Macromolecules* **2002**, *35*, 8418–8427. (f) Gudipaty, C. S.; Greenlief, C. M.; Johnson, J. A.; Wooley, K. L. *J. Polym. Sci., Part A: Polym. Chem.* **2004**, *42*, 6193–6208.

(3) (a) Christodoulakis, K. E.; Palioura, D.; Anastasiadis, S. H.; Vamvakaki, M. *Top. Catal.* **2009**, *52*, 394–411. (b) Li, Z. H.; Pan, Y.; Zhang, P.; Zheng, Z. H.; Ding, X. B.; Peng, Y. X. *e-Polym.* **2009**, no. 025. (c) Li, X. F.; Basko, M.; Du Prez, F.; Vankelecom, I. F. J. *J. Phys. Chem. B* **2008**, *112*, 16539–16545. (d) Reyntjens, G. W.; Jonckheere, L. E.; Goethals, E. J. *Macromol. Rapid Commun.* **2002**, *23*, 282–285. (e) Hentze, H.-P.; Krämer, E.; Berton, B.; Förster, S.; Antonietti, M.; Dreja, M. *Macromolecules* **1999**, *32*, 5803–5809. (f) Gitsov, I.; Zhu, C. *J. Am. Chem. Soc.* **2003**, *125*, 11228–11234. (g) Bartels, J. W.; Cheng, C.; Powell, K. T.; Wooley, K. L. *Macromol. Chem. Phys.* **2007**, *208*, 1676–1687.

(4) (a) Rimmer, S.; Wilshaw, S.-P.; Pickavance, P.; Ingham, E. *Biomaterials* **2009**, *30*, 2468–2478. (b) Ajiro, H.; Takemoto, Y.; Akashi, M. *Chem. Lett.* **2009**, *38*, 368–369. (c) Rakovsky, A.; Marbach, D.; Lotan, N.; Lanir, Y. *J. Appl. Polym. Sci.* **2009**, *112*, 390–401. (d) Erdodi, G.; Kang, J. M.; Yalcin, B.; Cakmak, M.; Rosenthal, K. S.; Grundfest-Broniatowski, S.; Kennedy, J. P. *Biomed. Microdevices* **2009**, *11*, 297–312. (e) Bromberg, L.; Temchenko, M.; Hatton, T. A. *Langmuir* **2002**, *18*, 4944–4952. (f) Tanahashi, K.; Jo, S.; Mikos, A. G. *Biomacromolecules* **2002**, *3*, 1030–1037. (g) Barakat, I.; Dubois, Ph.; Grandfils, Ch.; Jérôme, R. *J. Polym. Sci., Part A: Polym. Chem.* **1999**, *37*, 2401–2411. (h) Zhu, C.; Hard, C.; Lin, C.; Gitsov, I. *J. Polym. Sci., Part A: Polym. Chem.* **2005**, *43*, 4017–4029.

(5) Triftaridou, A. I.; Kafouris, D.; Vamvakaki, M.; Georgiou, T. K.; Krasia, T. C.; Themistou, E.; Hadjiantoniou, N.; Patrickios, C. S. *Polym. Bull.* **2007**, *58*, 185–190.

(6) (a) Simmons, M. R.; Yamasaki, E. N.; Patrickios, C. S. *Macromolecules* **2000**, *33*, 3176–3179. (b) Triftaridou, A. I.; Hadjiyannakou, S. C.; Vamvakaki, M.; Patrickios, C. S. *Macromolecules* **2002**, *35*, 2506–2513. (c) Krasia, T. C.; Patrickios, C. S. *Macromolecules* **2006**, *39*, 2467–2473. (d) Georgiou, T. K.; Patrickios, C. S.; Groh, P. W.; Iván, B. *Macromolecules* **2007**, *40*, 2335–2343. (e) Achilleos, M.; Krasia-Christoforou, T.; Patrickios, C. S. *Macromolecules* **2007**, *40*, 5575–5581. (f) Hadjiantoniou, N. A.; Patrickios, C. S. *Polymer* **2007**, *48*, 7041–7048. (g) Vamvakaki, M.; Patrickios, C. S. *Soft Matter* **2008**, *4*, 268–276. (h) Achilleos, M.; Legge, T. M.; Perrier, S.; Patrickios, C. S. *J. Polym. Sci., Part A: Polym. Chem.* **2008**, *46*, 7556–7565. (i) Kali, G.; Georgiou, T. K.; Iván, B.; Patrickios, C. S. *J. Polym. Sci., Part A: Polym. Chem.* **2009**, *47*, 4289–4301.

(7) (a) Kali, G.; Georgiou, T. K.; Iván, B.; Patrickios, C. S.; Loizou, E.; Thomann, Y.; Tiller, J. C. *Macromolecules* **2007**, *40*, 2192–2200. (b) Triftaridou, A. I.; Vamvakaki, M.; Patrickios, C. S. *Biomacromolecules* **2007**, *8*, 1615–1623. (c) Vamvakaki, M.; Patrickios, C. S.; Lindner, P.; Gradzielski, M. *Langmuir* **2007**, *23*, 10433–10437. (d) Kali, G.; Georgiou, T. K.; Iván, B.; Patrickios, C. S.; Loizou, E.; Thomann, Y.; Tiller, J. C. *Langmuir* **2007**, *23*, 10746–10755. (e) Triftaridou, A. I.; Loizou, E.; Patrickios, C. S. *J. Polym. Sci., Part A: Polym. Chem.* **2008**, *46*, 4420–4432. (f) Kafouris, D.; Gradzielski, M.; Patrickios, C. S. *Macromolecules* **2009**, *42*, 2972–2980. (g) Hadjiantoniou, N. A.; Patrickios, C. S.; Thomann, Y.; Tiller, J. C. *Macromol. Chem. Phys.* **2009**, *210*, 942–950.

(8) (a) Falco, E. E.; Patel, M.; Fisher, J. P. *Pharm. Res.* **2008**, *25*, 2348–2356. (b) Vert, M. *J. Mater. Sci.: Mater. Med.* **2009**, *20*, 437–446. (c) Bencherif, S. A.; Sheehan, J. A.; Hollinger, J. O.; Walker, L. M.; Matyjaszewski, K.; Washburn, N. R. *J. Biomed. Mater. Res., Part A* **2009**, *90*, 142–153.

(9) (a) Wiltshire, J. T.; Qiao, G. G. *Aust. J. Chem.* **2007**, *60*, 699–705. (b) Cho, E.; Kutty, J. K.; Dator, K.; Lee, J. S.; Vyavahare, N. R.; Webb, K. *J. Biomed. Mater. Res., Part A* **2009**, *90*, 1073–1082. (c) Metz, N.; Theato, P. *Macromolecules* **2009**, *42*, 37–39.

(10) (a) Themistou, E.; Patrickios, C. S. *J. Polym. Sci., Part A: Polym. Chem.* **2009**, *47*, 5853−5870.(b) Themistou, E.; Patrickios, C. S. *Macromol. Chem. Phys.* **2008**, *209*, 1021–1028. (c) Themistou, E.; Kanari, A.; Patrickios, C. S. *J. Polym. Sci., Part A: Polym. Chem.* **2007**, *45*, 5811–5823. (d) Themistou, E.; Patrickios, C. S. *Macromolecules* **2007**, *40*, 5231–5234. (e) Kafouris, D.; Themistou, E.; Patrickios, C. S. *Chem. Mater.* **2006**, *18*, 85–93. (f) Themistou, E.; Patrickios, C. S. *Macromolecules* **2006**, *39*, 73–80. (g) Themistou, E.; Patrickios, C. S. *Macromolecules* **2004**, *37*, 6734–6743.

(11) (a) Tsarevsky, N. V.; Matyjaszewski, K. *Macromolecules* **2002**, *35*, 9009–9014. (b) Tsarevsky, N. V.; Matyjaszewski, K. *Macromolecules* **2005**, *38*, 3087–3092. (c) Li, C.; Madsen, J.; Armes, S. P.; Lewis, A. L. *Angew. Chem., Int. Ed.* **2006**, *45*, 3510–3513. (d) Johnson, J. A.; Lewis, D. R.; Díaz, D. D.; Finn, M. G.; Koberstein, J. T.; Turro, N. J. *J. Am. Chem. Soc.* **2006**, *128*, 6564–6565. (e) Johnson, J. A.; Finn, M. G.; Koberstein, J. T.; Turro, N. J. *Macromolecules* **2007**, *40*, 3589–3598. (f) He, T.; Adams, D. J.; Butler, M. F.; Cooper, A. I.; Rannard, S. P. *J. Am. Chem. Soc.* **2009**, *131*, 1495–1501.

(12) (a) Wang, J.-S.; Matyjaszewski, K. *J. Am. Chem. Soc.* **1995**, *117*, 5614–5615. (b) Matyjaszewski, K.; Xia, J. *Chem. Rev.* **2001**, *101*, 2921–2990.

(13) (a) Webster, O. W.; Hertler, W. R.; Sogah, D. Y.; Farnham, W. B.; RajanBabu, T. V. *J. Am. Chem. Soc.* **1983**, *105*, 5706–5708. (b) Sogah, D. Y.; Hertler, W. R.; Webster, O. W.; Cohen, G. M. *Macromolecules* **1987**, *20*, 1473–1488. (c) Webster, O. W. *J. Polym. Sci., Part A: Polym. Chem.* **2000**, *38*, 2855–2860. (d) Webster, O. W. *Adv. Polym. Sci.* **2004**, *167*, 1–34. (e) Raynaud, J.; Ciolino, J.; Baceiredo, A.; Destarac, M.; Bonnette, F.; Kato, T.; Gnanou, Y.; Taton, D. *Angew. Chem., Int. Ed.* **2008**, *47*, 5390–5393. (f) Raynaud, J.; Gnanou, Y.; Taton, D. *Macromolecules* **2009**, *42*, 5996–6005.

(14) Dicker, I. B.; Cohen, G. M.; Farnham, W. B.; Hertler, W. R.; Laganis, E. D.; Sogah, D. Y. *Macromolecules* **1990**, *23*, 4034–4041.

(15) Rikkou, M. D.; Patrickios, C. S. *Macromolecules* **2008**, *41*, 5957–5959.

(16) (a) Mespouille, L.; Coulembier, O.; Paneva, D.; Degée, P.; Rashkov, I.; Dubois, Ph. *Chem.—Eur. J.* **2008**, *14*, 6369–6378. (b) Zednik, J.; Riva, R.; Lussis, P.; Jérôme, C.; Jérôme, R.; Lecomte, P. *Polymer* **2008**, *49*, 697–702.

(17) (a) Hoogenboom, R.; Schubert, U. S.; Van Camp, W.; Du Prez, F. E. *Macromolecules* **2005**, *38*, 7653–7659. (b) Otsuka, H.; Endo, T. *Macromolecules* **1999**, *32*, 9059–9061.

(18) Vanwetswinkel, S.; Carlier, V.; Marchand-Brynaert, J.; Fastrez, J. *Tetrahedron Lett.* **1996**, *37*, 2761–2762.